Biomedical Optics EXPRESS

Precancerous esophageal epithelia are associated with significantly increased scattering coefficients

Jing-Wei Su,[1] Yang-Hsien Lin,[1] Chun-Ping Chiang,[2,7] Jang-Ming Lee,[3,7] Chao-Mao Hsieh,[1] Min-Shu Hsieh,[4,7] Pei-Wen Yang,[3,7] Chen-Ping Wang,[5,7] Ping-Huei Tseng,[6,7] Yi-Chia Lee,[6,7] and Kung-Bin Sung[1,8,9,*]

[1]Institute of Biomedical Electronics and Bioinformatics, National Taiwan University, Taiwan
[2]Department of Dentistry, National Taiwan University Hospital, Taiwan
[3]Department of Surgery, National Taiwan University Hospital, Taiwan
[4]Department of Pathology, National Taiwan University Hospital, Taiwan
[5]Department of Otolaryngology, National Taiwan University Hospital, Taiwan
[6]Department of Internal Medicine, National Taiwan University Hospital, Taiwan
[7]National Taiwan University College of Medicine, Taiwan
[8]Department of Electrical Engineering, National Taiwan University, Taiwan
[9]Molecular Imaging Center, National Taiwan University, Taiwan
[*]kbsung@ntu.edu.tw

Abstract: The progression of epithelial precancers into cancer is accompanied by changes of tissue and cellular structures in the epithelium. Correlations between the structural changes and scattering coefficients of esophageal epithelia were investigated using quantitative phase images and the scattering-phase theorem. An *ex vivo* study of 14 patients demonstrated that the average scattering coefficient of precancerous epithelia was 37.8% higher than that of normal epithelia from the same patient. The scattering coefficients were highly correlated with morphological features including the cell density and the nuclear-to-cytoplasmic ratio. A high interpatient variability in scattering coefficients was observed and suggests identifying precancerous lesions based on the relative change in scattering coefficients.

OCIS codes: (170.6935) Tissue characterization; (170.4580) Optical diagnostics for medicine; (170.0180) Microscopy; (290.7050) Turbid media.

References and links

1. T. Collier, M. Follen, A. Malpica, and R. Richards-Kortum, "Sources of scattering in cervical tissue: determination of the scattering coefficient by confocal microscopy," Appl. Opt. **44**(11), 2072–2081 (2005).
2. V. Backman, M. B. Wallace, L. T. Perelman, J. T. Arendt, R. Gurjar, M. G. Müller, Q. Zhang, G. Zonios, E. Kline, J. A. McGilligan, S. Shapshay, T. Valdez, K. Badizadegan, J. M. Crawford, M. Fitzmaurice, S. Kabani, H. S. Levin, M. Seiler, R. R. Dasari, I. Itzkan, J. Van Dam, and M. S. Feld, "Detection of preinvasive cancer cells," Nature **406**(6791), 35–36 (2000).
3. D. Arifler, M. Guillaud, A. Carraro, A. Malpica, M. Follen, and R. Richards-Kortum, "Light scattering from normal and dysplastic cervical cells at different epithelial depths: finite-difference time-domain modeling with a perfectly matched layer boundary condition," J. Biomed. Opt. **8**(3), 484–494 (2003).
4. R. Drezek, M. Guillaud, T. Collier, I. Boiko, A. Malpica, C. Macaulay, M. Follen, and R. Richards-Kortum, "Light scattering from cervical cells throughout neoplastic progression: influence of nuclear morphology, DNA content, and chromatin texture," J. Biomed. Opt. **8**(1), 7–16 (2003).
5. J. D. Rogers, A. J. Radosevich, J. Yi, and V. Backman, "Modeling Light Scattering in Tissue as Continuous Random Media Using a Versatile Refractive Index Correlation Function," IEEE J. Sel. Top. Quantum Electron. **20**(2), 7000514 (2013).
6. J. D. Rogers, İ. R. Capoğlu, and V. Backman, "Nonscalar elastic light scattering from continuous random media in the Born approximation," Opt. Lett. **34**(12), 1891–1893 (2009).
7. A. Taflove and S. C. Hagness, "FDTD Modeling Applications," in Computational Electrodynamics: The Finite-Difference Time-Domain 3ed. (Artech House, 2005).
8. M. Xu, "Scattering-phase theorem: anomalous diffraction by forward-peaked scattering media," Opt. Express **19**(22), 21643–21651 (2011).
9. Z. Wang, H. Ding, and G. Popescu, "Scattering-phase theorem," Opt. Lett. **36**(7), 1215–1217 (2011).

#245779 Received 10 Jul 2015; revised 28 Aug 2015; accepted 31 Aug 2015; published 3 Sep 2015

10. Z. Wang, K. Tangella, A. Balla, and G. Popescu, "Tissue refractive index as marker of disease," J. Biomed. Opt. **16**(11), 116017 (2011).
11. D. Levitz, L. Thrane, M. Frosz, P. Andersen, C. Andersen, S. Andersson-Engels, J. Valanciunaite, J. Swartling, and P. Hansen, "Determination of optical scattering properties of highly-scattering media in optical coherence tomography images," Opt. Express **12**(2), 249–259 (2004).
12. D. Faber, F. van der Meer, M. Aalders, and T. van Leeuwen, "Quantitative measurement of attenuation coefficients of weakly scattering media using optical coherence tomography," Opt. Express **12**(19), 4353–4365 (2004).
13. K. A. Vermeer, J. Mo, J. J. A. Weda, H. G. Lemij, and J. F. de Boer, "Depth-resolved model-based reconstruction of attenuation coefficients in optical coherence tomography," Biomed. Opt. Express **5**(1), 322–337 (2014).
14. I. V. Turchin, E. A. Sergeeva, L. S. Dolin, V. A. Kamensky, N. M. Shakhova, and R. Richards-Kortum, "Novel algorithm of processing optical coherence tomography images for differentiation of biological tissue pathologies," J. Biomed. Opt. **10**(6), 064024 (2005).
15. O. K. Adegun, P. H. Tomlins, E. Hagi-Pavli, G. McKenzie, K. Piper, D. L. Bader, and F. Fortune, "Quantitative analysis of optical coherence tomography and histopathology images of normal and dysplastic oral mucosal tissues," Lasers Med. Sci. **27**(4), 795–804 (2012).
16. T. Collier, M. Guillaud, M. Follen, A. Malpica, and R. Richards-Kortum, "Real-time reflectance confocal microscopy: comparison of two-dimensional images and three-dimensional image stacks for detection of cervical precancer," J. Biomed. Opt. **12**(2), 024021 (2007).
17. A. L. Clark, A. Gillenwater, R. Alizadeh-Naderi, A. K. El-Naggar, and R. Richards-Kortum, "Detection and diagnosis of oral neoplasia with an optical coherence microscope," J. Biomed. Opt. **9**(6), 1271–1280 (2004).
18. D. Arifler, C. Macaulay, M. Follen, and M. Guillaud, "Numerical investigation of two-dimensional light scattering patterns of cervical cell nuclei to map dysplastic changes at different epithelial depths," Biomed. Opt. Express **5**(2), 485–498 (2014).
19. J. Q. Brown, K. Vishwanath, G. M. Palmer, and N. Ramanujam, "Advances in quantitative UV-visible spectroscopy for clinical and pre-clinical application in cancer," Curr. Opin. Biotechnol. **20**(1), 119–131 (2009).
20. C. C. Yu, C. Lau, G. O'Donoghue, J. Mirkovic, S. McGee, L. Galindo, A. Elackattu, E. Stier, G. Grillone, K. Badizadegan, R. R. Dasari, and M. S. Feld, "Quantitative spectroscopic imaging for non-invasive early cancer detection," Opt. Express **16**(20), 16227–16239 (2008).
21. S. Hariri Tabrizi, S. Mahmoud Reza Aghamiri, F. Farzaneh, A. Amelink, and H. J. Sterenborg, "Single fiber reflectance spectroscopy on cervical premalignancies: the potential for reduction of the number of unnecessary biopsies," J. Biomed. Opt. **18**(1), 017002 (2013).
22. K. B. Sung, K. W. Shih, F. W. Hsu, H. P. Hsieh, M. J. Chuang, Y. H. Hsiao, Y. H. Su, and G. H. Tien, "Accurate extraction of optical properties and top layer thickness of two-layered mucosal tissue phantoms from spatially resolved reflectance spectra," J. Biomed. Opt. **19**(7), 077002 (2014).
23. Q. Wang, D. Le, J. Ramella-Roman, and J. Pfefer, "Broadband ultraviolet-visible optical property measurement in layered turbid media," Biomed. Opt. Express **3**(6), 1226–1240 (2012).
24. C. Redden Weber, R. A. Schwarz, E. N. Atkinson, D. D. Cox, C. Macaulay, M. Follen, and R. Richards-Kortum, "Model-based analysis of reflectance and fluorescence spectra for in vivo detection of cervical dysplasia and cancer," J. Biomed. Opt. **13**(6), 064016 (2008).
25. Q. Liu and N. Ramanujam, "Sequential estimation of optical properties of a two-layered epithelial tissue model from depth-resolved ultraviolet-visible diffuse reflectance spectra," Appl. Opt. **45**(19), 4776–4790 (2006).
26. J. W. Su, W. C. Hsu, C. Y. Chou, C. H. Chang, and K. B. Sung, "Digital holographic microtomography for high-resolution refractive index mapping of live cells," J. Biophotonics **6**(5), 416–424 (2013).
27. Z. Wang and B. Han, "Advanced iterative algorithm for phase extraction of randomly phase-shifted interferograms," Opt. Lett. **29**(14), 1671–1673 (2004).
28. Y. C. Lee, C. P. Wang, C. C. Chen, H. M. Chiu, J. Y. Ko, P. J. Lou, T. L. Yang, H. Y. Huang, M. S. Wu, J. T. Lin, T. Hsiu-Hsi Chen, and H. P. Wang, "Transnasal endoscopy with narrow-band imaging and Lugol staining to screen patients with head and neck cancer whose condition limits oral intubation with standard endoscope (with video)," Gastrointest. Endosc. **69**(3), 408–417 (2009).
29. Y. C. Lee, H. P. Wang, C. P. Wang, J. Y. Ko, J. M. Lee, H. M. Chiu, J. T. Lin, S. Yamashita, D. Oka, N. Watanabe, Y. Matsuda, T. Ushijima, and M. S. Wu, "Revisit of field cancerization in squamous cell carcinoma of upper aerodigestive tract: better risk assessment with epigenetic markers," Cancer Prev. Res. (Phila.) **4**(12), 1982–1992 (2011).
30. G. S. Chao and K. B. Sung, "Investigating the spectral characteristics of backscattering from heterogeneous spherical nuclei using broadband finite-difference time-domain simulations," J. Biomed. Opt. **15**(1), 015007 (2010).
31. I. R. Capoğlu, J. D. Rogers, A. Taflove, and V. Backman, "Accuracy of the Born approximation in calculating the scattering coefficient of biological continuous random media," Opt. Lett. **34**(17), 2679–2681 (2009).
32. J. W. Su, W. C. Hsu, J. W. Tjiu, C. P. Chiang, C. W. Huang, and K. B. Sung, "Investigation of influences of the paraformaldehyde fixation and paraffin embedding removal process on refractive indices and scattering properties of epithelial cells," J. Biomed. Opt. **19**(7), 075007 (2014).
33. J. R. Mourant, T. Fuselier, J. Boyer, T. M. Johnson, and I. J. Bigio, "Predictions and measurements of scattering and absorption over broad wavelength ranges in tissue phantoms," Appl. Opt. **36**(4), 949–957 (1997).

#245779 Received 10 Jul 2015; revised 28 Aug 2015; accepted 31 Aug 2015; published 3 Sep 2015

1. Introduction

Dysplasia is a histological precursor of cancers originating from stratified squamous epithelia. The cancerization is often accompanied by subcellular structural transformation such as enlarged nuclei, an increased nuclear-to-cytoplasmic ratio (N/C), and irregularly shaped and hyperchromatic nuclei in the epithelium [1–3]. These features are used to identify precancerous lesions in current histopathological diagnoses for which part of the tissue shall be removed.

Many studies have indicated that dysplastic progression changes the light scattering properties of cellular structures such as rises in total scattering cross-section and backscattering cross-section [3–7]. The Richards-Kortum group has applied a rigorous numerical electromagnetic technique, the finite-difference time-domain (FDTD) method, to calculate the scattering properties of individual cell nuclei and cells of the cervical epithelium [3,4]. The studies have concluded that the total scattering cross-sections and backscattering of epithelial cells increase with the development of dysplasia. Alternatively, the Backman group has modeled the refractive-index (RI) distributions of biological tissue with the Whittle–Matérn correlation function based on electron microscopic images and derived the correlation between the numerical tissue model and scattering coefficients [5,6]. The previous studies provide valuable insights into the correlations between structures and scattering properties of soft tissue. However, the actual RI values and distributions of cellular structures in the epithelium are unknown. Therefore, these numerical methods are not suitable to quantify the scattering coefficients of real tissue specimens.

In order to estimate the scattering properties of tissue specimens, Wang *et al*. and Xu have proposed a scattering-phase theorem to estimate the scattering coefficients and anisotropy factors of thin tissue slices from quantitative phase images of the slices [8,9]. The results of a preliminary study demonstrated that the malignant prostate tissue had higher scattering coefficients than normal tissue [10]. This promising method has not been used for investigating the differences in scattering coefficients between normal and precancerous epithelia until now.

A few techniques have been proposed to experimentally estimate the scattering coefficient of the epithelium for the *in vivo* diagnosis of precancers. Reflectance confocal microscopy [1] and optical coherence tomography [11–15] have been used to estimate the scattering coefficients of cervical and oral epithelia by fitting the depth-dependent decay of the singly backscattered light. The results suggest that the scattering coefficient is a promising biomarker for differentiating precancerous dysplasia from low-grade dysplasia or normal tissue [14–17]. However, the assumptions that the backscattering cross-section remains constant throughout the epithelial thickness may not be valid [18], rendering the estimation of scattering coefficients unreliable. Another group of techniques rely on detecting multiply scattered light which is also known as diffuse reflectance to estimate an average scattering coefficient of the tissue based on the radiative transport equation or Monte Carlo simulations for photon migration [19–21]. There have been recent efforts to estimate the scattering coefficient of the relatively thin epithelial layer in addition to the conventional estimation of the scattering and absorption coefficients of the semi-infinitely thick stromal layer [22–25]. Although promising, the methods have not achieved accurate extraction of the scattering coefficient of the epithelium *in vivo*.

The objective of this study is to quantify the scattering coefficients of normal and dysplastic epithelia in *ex vivo* esophageal specimens and determine the feasibility of using the scattering coefficient as a biomarker for precancerous epithelium. We quantified two-dimensional (2-D) phase images and three-dimensional (3-D) RI distributions of esophageal tissue slices using digital holographic microtomography (DHμT), and estimated the scattering coefficients of the epithelia by the scattering-phase theorem. The correlations between the tissue morphology, RI distribution and scattering coefficient were investigated.

#245779 Received 10 Jul 2015; revised 28 Aug 2015; accepted 31 Aug 2015; published 3 Sep 2015

2. Methods and materials

2.1 Instrumentation: digital holographic microtomography (DHμT)

We acquired 2-D phase images of tissue slices using DHμT which is essentially an imaging phase-shifting Mach-Zehnder interferometer [26]. Briefly, the output beam of a 532 nm continuous-wave diode-pumped solid-state laser was expanded before being divided into sample and reference beams. A piezoelectric actuator generated random phase shifts between the two beams. The sample beam was arranged to make plane-wave illumination on a transparent specimen. The transmitted and forwardly scattered field of the specimen was collected by an objective lens (Olympus UPLSAPO 100 XO, 1.4 NA) and recombined with a uniform reference beam to form interference images of the specimen, which were acquired by a high-speed CMOS camera (Point Grey Co.; Gazelle GZL-CL-41C6M-C) with a transverse magnification of about 85. A so-called advanced iterative algorithm was implemented to simultaneously retrieve the phase shifts and a quantitative phase image of the specimen from six interferograms [27]. For 3-D RI imaging, two galvanometer-based scanning mirrors were rotated to change the incident angle of the sample beam upon the specimen and 2-D phase images acquired within the angles of ± 65° were used to reconstruct a 3-D RI distribution of the specimen based on optical diffraction tomography [26]. The measured spatial resolution was approximately 0.35 μm in both axial and transverse dimensions.

2.2 Preparation of samples

We obtained histologically normal and precancerous esophageal epithelial tissue specimens from 14 patients diagnosed with upper aerodigestive tract cancer (squamous cell carcinoma). The specimens were taken before any chemo-irradiation. This study was approved by an Institutional Review Board of National Taiwan University Hospital, and informed consent was obtained from the subjects. The enrollment procedure has been previously reported [28,29]. For each patient, two or three fresh esophageal specimens taken from different sites of the esophagus were embedded in paraffin. For each paraffin-embedded tissue specimen, two adjacent 4 μm-thick slices were cut with a Leica RM2125 rotary microtome (Leica Microsysthems, Wetzlar, Germany) and laid on two separate glass slides. The tissue slices were deparaffinized with xylene and hydrated with an alcohol gradient (100%, 95%, 85%, 75% and 50%). One of the slices was immersed in phosphate buffered saline to measure 2-D phase images of the tissue slice using DHμT. The other slice was stained with hematoxylin and eosin (H&E) for pathological diagnosis given by a certified pathologist (CPC).

2.3 The scattering-phase theorem and validation

The scattering-phase theorem was used to estimate the scattering coefficients of esophageal epithelia from selected areas. According to the scattering-phase theorem, the light progression in a thin slice of forward-peaked scattering medium can be described by anomalous diffraction. If the slice thickness is much less than the inverse of the scattering coefficient, the scattering coefficient and reduced scattering coefficients are expressed as [8]

$$\mu_s = \frac{2\left\langle 1-\cos\left[\Delta\phi(x,y)\right]\right\rangle}{L}, \tag{1}$$

and

$$\mu_s^{'} = \frac{\left\langle \left|\nabla\phi(x,y)\right|^2 \right\rangle}{2L\cdot k^2}, \tag{2}$$

where L is the slice thickness, $\left\langle \Delta\phi(x,y)\right\rangle$ is the spatial average of phase fluctuations, and $\left\langle \left|\nabla\phi(x,y)\right|^2 \right\rangle$ is the spatial average of the phase gradient intensity [9]. The $k = 2\pi n_0/\lambda$ term is

#245779 Received 10 Jul 2015; revised 28 Aug 2015; accepted 31 Aug 2015; published 3 Sep 2015

the wave number, n_0 is the average refractive index of the medium, and λ is the wavelength of the light source. Anisotropy factor, g, can be computed as $g = 1 - \left(\mu_s^{'} / \mu_s \right)$.

To validate the accuracy of the scattering-phase theorem, we calculated the scattering coefficients of tissue slices by the FDTD method to provide a gold standard. The 3-D RI distribution of the esophageal epithelium with a size of 30 μm × 30 μm × 3.1 μm was obtained by DHμT and fed into home-made FDTD software [30] to calculate the differential scattering cross-sections at wavelengths ranging from 400 nm to 700 nm. The scattering coefficient of the tissue slice was calculated as [31]

$$\mu_s = \frac{1}{V} \int_{4\pi} \sigma_d d\Omega, \tag{3}$$

where σ_d is the differential scattering cross-section with the dimension of areas per solid angle and V is the tissue volume. σ_d is equal to the absolute square of the scattering amplitude calculated by the FDTD software.

2.4 Analysis of scattering coefficients of esophageal epithelia

Using the scattering-phase theorem to calculate the scattering coefficients of epithelial tissue requires the tissue cut into thin slices. A previous study showed that the processes of fixation and paraffin embedding, which are necessary for cutting thin tissue slices, change not only the cellular RI but also the morphology [32]. As a result, the scattering coefficients increase significantly due to the shrinkage of volume and the increased standard deviation of RI. Before applying the scattering-phase theorem to estimate the scattering coefficients of fresh or *in vivo* epithelial tissue from tissue slices, we compensated for the volume shrinkage by expanding the length, width and thickness of the tissue slices with the same factor of 1.12, which is the cube root of the tissue volume shrinkage ratio. The volume shrinkage ratio was estimated by comparing the average cellular volume of fresh oral epithelial tissue to that of the same specimen after the specimen was paraffinized, cut into thin slices and deparaffinized [32]. The change in the standard deviation of the phase due to the paraffin embedding-removal process was previously investigated *in vitro* by comparing the 3-D RI images of the same epithelial cells before and after the fixation and paraffin embedding-removal processes. It was found that the standard deviations of RI increased by an average factor of 2.11 [32]. In the current study the standard deviation of the phase distribution of every selected epithelial area was divided by 2.11 to compensate for the influences of fixation and paraffin embedding-removal.

For the ease of calculation using Eq. (1) and Eq. (2), the epithelial layer was divided into 30-μm wide rectangular regions of interest (Fig. 1) and the physical thickness of the slices was verified by the 3-D RI distribution obtained with DHμT. We investigated the epithelial tissue in two groups based on the pathological diagnoses: the normal group including normal and mild dysplasia, and the precancerous group including moderate dysplasia and severe dysplasia. Mild dysplasia is considered non-dysplastic because it has low risk to develop into cancer and is recommended to be checked by follow-up endoscopic examinations.

#245779 Received 10 Jul 2015; revised 28 Aug 2015; accepted 31 Aug 2015; published 3 Sep 2015

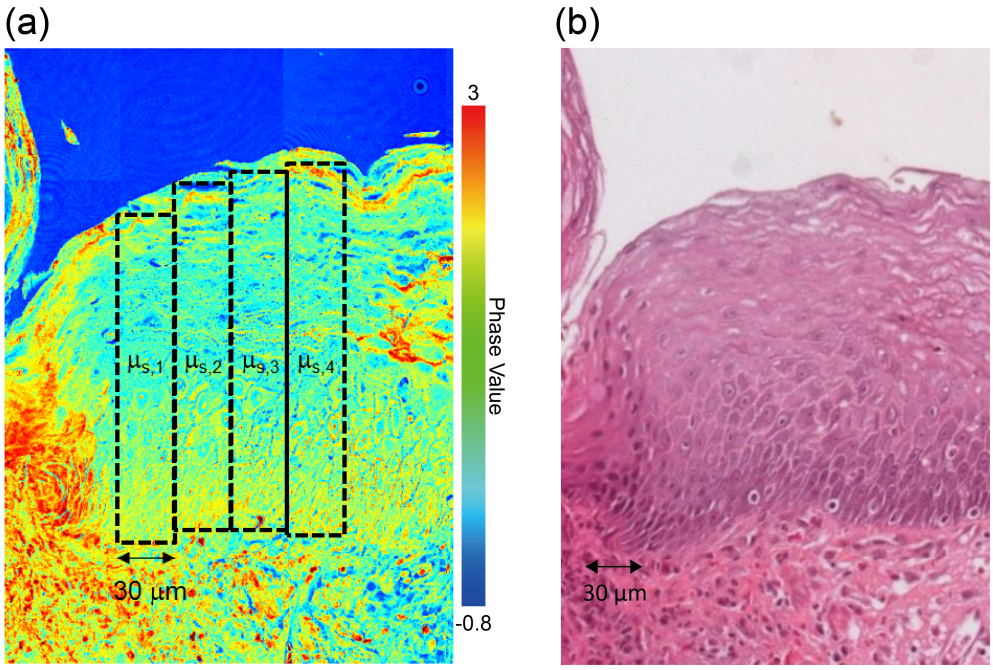

Fig. 1. Examples of (a) a phase image of the unstained slice, and (b) a bright-field image of the H&E stained slice from the same esophageal specimen. Selected rectangular regions for the scattering-coefficient analysis are indicated with dashed lines in (a).

3. Results

3.1 Scattering coefficients calculated by FDTD and scattering-phase theorem

A representative 3-D RI distribution of a 30 μm × 30 μm × 3.1 μm region of the esophageal epithelium is show in Fig. 2(a). The results in Fig. 2(b) show that the wavelength-dependent scattering coefficients obtained using Eq. (1) are consistent with those obtained with the FDTD simulation. The percentage deviation between the scattering coefficients calculated with the two methods was 5.1%.

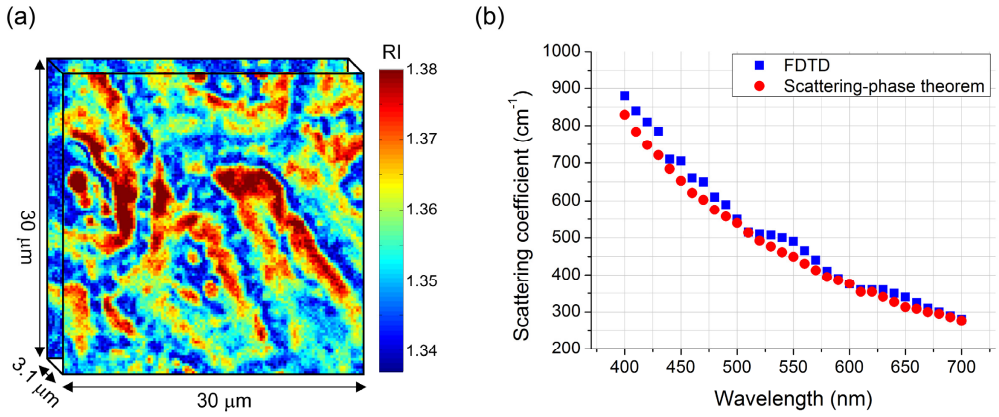

Fig. 2. Results of verifying the accuracy of estimating the scattering coefficients of esophageal epithelium by the scattering-phase theorem: (a) 3-D RI distribution, and (b) the scattering coefficients calculated with the FDTD method (blue squares) and the scattering-phase theorem (red circles).

#245779 Received 10 Jul 2015; revised 28 Aug 2015; accepted 31 Aug 2015; published 3 Sep 2015

3.2 Statistical analysis of scattering coefficients and anisotropy factors

The statistical results of the scattering coefficients and anisotropy factors of the normal and precancerous regions of each patient are summarized in Fig. 3. The mean (open squares), median (central line of the boxes), minimum and maximum values (crosses) as well as the first and third quartiles (the bottom and the top edges of the boxes respectively) are shown. The ends of the whiskers represent the minimum and maximum values which are not outliers. For each patient the precancerous epithelia showed noticeably higher scattering coefficients than the normal epithelia. The anisotropy factors of precancerous epithelia were slightly higher than those of the normal epithelia in all patients except for patients No. 3 and No. 14. The average intrapatient differences in the scattering coefficient and anisotropy factor between the precancerous and normal regions were 37.8% and 2.0%, respectively. Overall, the average scattering coefficients of normal and precancerous epithelia of the 14 patients were 152 ± 42 cm^{-1} and 206 ± 54 cm^{-1}, respectively. The average anisotropy factors of normal and precancerous epithelia were 0.946 ± 0.028 and 0.964 ± 0.034, respectively. We then applied the one-tailed Student's t-test to determine whether the differences were significant. The results demonstrate that for all the selected regions (N = 320) the scattering coefficients of the precancerous regions were significantly higher ($p<0.001$) than those of the normal regions. The anisotropy factors of the precancerous regions were also significantly higher ($p<0.01$) than those of the normal regions. Note that there were very high interpatient variabilities in the scattering coefficients and anisotropy factors of both the normal and precancerous epithelia (more results in Section 3.4).

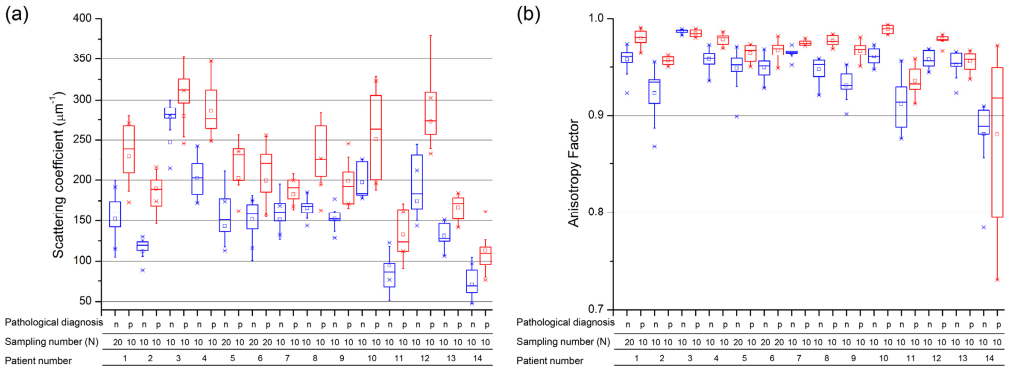

Fig. 3. Box-and-whisker plot showing the scattering coefficients and anisotropic factors of normal and precancerous esophageal epithelia. For each patient the average scattering coefficient of the precancerous epithelia (red) was significantly higher than that of the normal epithelia (blue).

3.3 Correlation between scattering coefficients, cell density and N/C

In order to investigate the correlation between morphological features and scattering coefficients of the epithelium, the cell density and the N/C of the selected regions were calculated based on images of the corresponding H&E stained slices. Representative bright-field images and phase images of normal and precancerous epithelia from the same patient are shown in Fig. 4(a)-4(d). Figure 4(e)-4(g) show the localized scattering coefficient, cell density and N/C at various depths of the epithelial layer, respectively. Figure 4(e) illustrates that the lower one-third of the normal epithelium (diagnosed as mild dysplasia according to histopathology) had higher scattering coefficients, while in the precancerous epithelium (diagnosed as moderate dysplasia) the lower half of the epithelium showed elevated scattering coefficients. Similar trends can be seen in the cell density and N/C as shown in Fig. 4(f) and 4(g), i.e. the precancerous epithelium showing higher cell density and N/C than the normal epithelium *in the intermediate layers*. The trends in cell density and N/C are consistent with the well-known histological hallmarks of normal and precancerous stratified squamous

#245779 Received 10 Jul 2015; revised 28 Aug 2015; accepted 31 Aug 2015; published 3 Sep 2015

epithelia. Furthermore, we calculated the Pearson's correlation coefficients to quantify the correlation of the scattering coefficient to the cell density and N/C. The correlation coefficient between the cell density and scattering coefficient was 0.90 and the correlation coefficient between the N/C and scattering coefficient was 0.85. The results demonstrate that for the same patient the scattering coefficients of esophageal epithelia are highly correlated with the cell density and N/C.

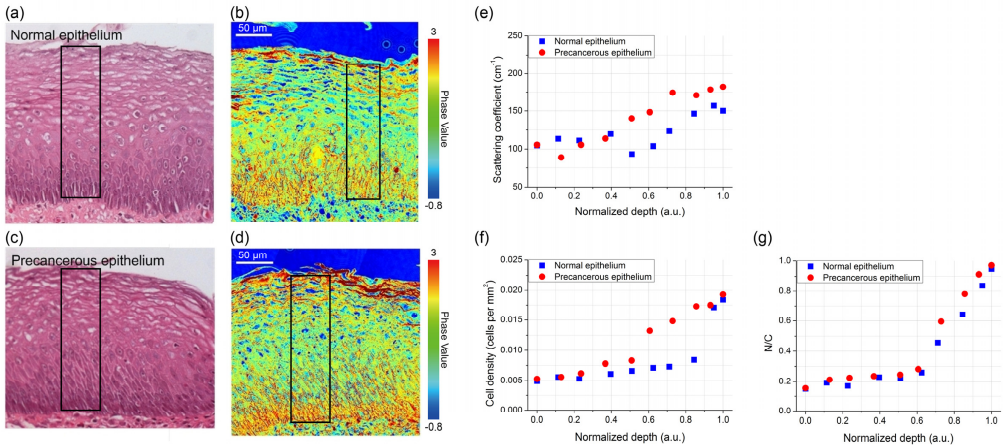

Fig. 4. Illustration of the scattering coefficient, cell density and N/C ratio. (a) and (c) are brightfield images of the H&E stained normal and precancerous epithelia, respectively. (b) and (d) are the corresponding phase images. (e), (f) and (g) are the depth-dependent scattering coefficient, cell density and N/C respectively of the selected regions (black solid lines) in (a)-(d).

3.4 Scattering coefficients of different patients

We further investigated the high interpatient variability in the scattering coefficient. Figure 5(a) shows the phase images of normal epithelia from two patients. Although the two normal epithelial regions have similar cell densities, the distributions of RI are significantly different as shown in Fig. 5(b), resulting in the high diversity of scattering coefficients in different patients shown in Fig. 3. The average cell densities and average scattering coefficients of both the normal and precancerous epithelia from each of the 14 patients are compared in a scatter plot (Fig. 6). The per-patient average cell density and average scattering coefficient show no correlation. The N/C is a similar morphologic feature to the cell density because images of the epithelia showed no significant change in the nuclear size between the normal and precancerous regions (data not shown). The results suggest that RI distributions differ significantly between individuals and dominate the scattering coefficients. The cause of the different RI distributions between patients is unknown and needs further research.

#245779 Received 10 Jul 2015; revised 28 Aug 2015; accepted 31 Aug 2015; published 3 Sep 2015

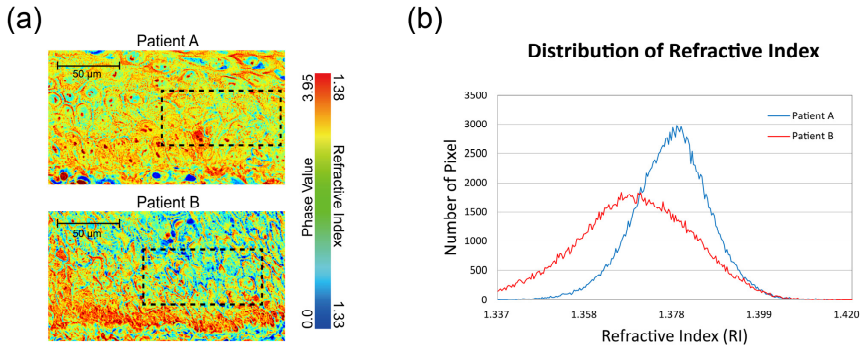

Fig. 5. Comparison of the epithelial phase and RI distributions between two patients. (a) Phase/RI images of normal epithelia from patients A and B. (b) Distributions of the RI of the selected regions (black dashed lines) in (a). The average RI of patient A and B are 1.378 ± 0.009 and 1.369 ± 0.014, respectively.

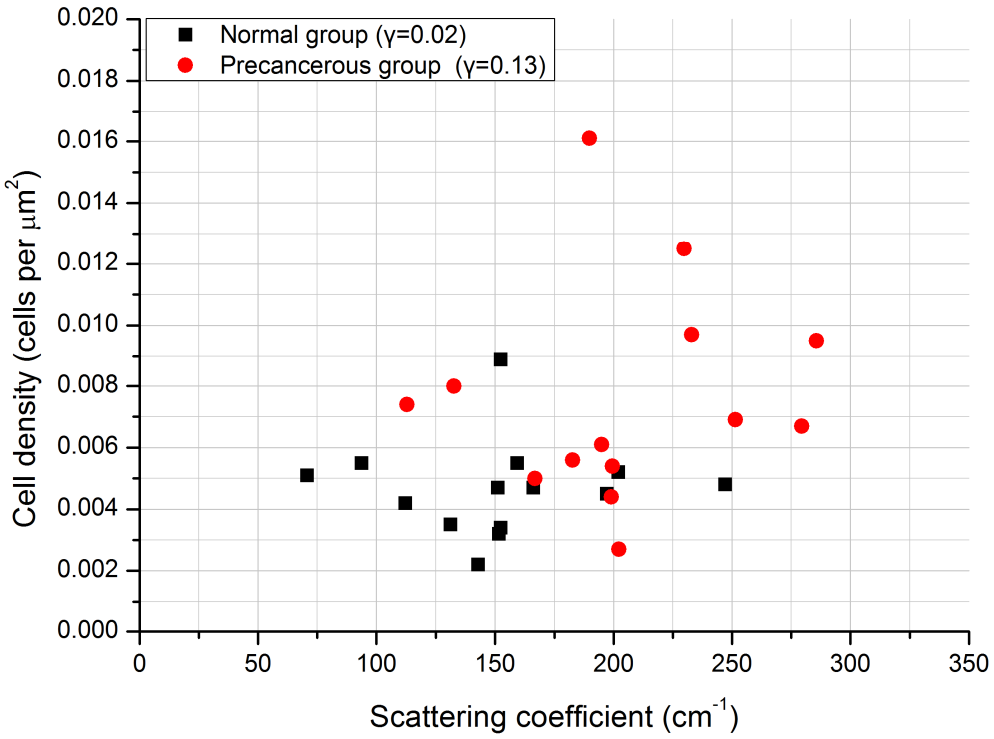

Fig. 6. Illustration of the correlation between per-patient average scattering coefficient and average cell density of the 14 patients. The correlation coefficients (γ) between the average scattering coefficients and the average cell densities are 0.02 and 0.13 for the normal and precancerous group, respectively.

4. Discussion and conclusion

The current study estimated the scattering coefficients of esophageal epithelia from *ex vivo* tissue slices. The effects of the histological processing on the refractive index and structure of the tissue were compensated for according to a previous study [32]. Specimens taken from different patients may have gone through slightly different processing, which could partly contribute to the high interpatient variability in the estimated scattering coefficients. For

#245779 Received 10 Jul 2015; revised 28 Aug 2015; accepted 31 Aug 2015; published 3 Sep 2015

specimens taken from the same patient the variability in specimen processing would be minimal. Therefore, the 37.8% intrapatient increase in scattering coefficients and 2.0% increase in anisotropy factors between precancerous and normal epithelia (Fig. 3) reflects changes in tissue structure and morphology that are associated with the progression of dysplasia. Influences of risk factors for esophageal cancer such as age, gender, tobacco smoking and alcohol consumption were not analyzed due to the limited size of samples in this pilot study.

We hypothesized that the increased cell density and N/C are the main sources of the significantly increased scattering coefficients in precancerous epithelia. In order to support this hypothesis, we investigated the scattering coefficients of normal and precancerous epithelia with similar structures (i.e. in the superficial layers or the basal layers). The scattering coefficients of the superficial layers in the normal and precancerous areas were 90 ± 15 cm^{-1} and 93 ± 11 cm^{-1}, respectively. The scattering coefficients of the basal layers in the normal and precancerous areas were 137 ± 16 cm^{-1} and 135 ± 17 cm^{-1}, respectively. The basal layer showed significantly higher scattering coefficients than the superficial layers ($p<0.001$), which is also demonstrated in Fig. 4(e). Normal and precancerous epithelia showed no differences in scattering coefficients in either superficial or basal layers. The results demonstrate that the morphology may be a primary factor to affect the scattering coefficient. According to the electromagnetic theory elastic light scattering is caused by inhomogeneous distribution of RI. One can see in the RI images of the epithelia (Figs. 4 and 5) that the nucleolus, the part of the cytoplasm surrounding the nucleus and the junction between cells generate the most contrast in RI. During the development of dysplasia cube-shaped cells that resemble basal cells with a higher density and N/C gradually take the places of extended cells in the intermediate and superficial layers. Therefore, precancerous epithelia have denser high RI-contrast structures and thus higher average scattering coefficients than normal epithelia.

Previous studies have investigated scattering coefficients of the epithelial tissue in organs including the oral cavity, uterine cervix and the skin, but the esophageal epithelium has not been explored. A previous reflectance confocal study investigated the scattering coefficients of *ex vivo* cervical epithelia after verifying that the reflectivity of nuclei, the main source of image contrast, was approximately constant throughout the epithelial thickness [16]. The study estimated the scattering coefficients at 810-nm wavelength to be 20-50 cm^{-1} in normal/low-grade epithelia and 55-150 cm^{-1} in precancerous epithelia. The scattering coefficients of normal and precancerous esophageal epithelia estimated by the current study are for the wavelength of 532 nm and can be transformed to be 100 cm^{-1} and 135 cm^{-1} respectively for the wavelength of 810 nm, assuming that the scattering coefficient follows wavelength dependence of λ^{-1} [33]. Both studies indicate significantly increased scattering coefficients in precancerous epithelia. The scattering coefficients estimated by the current study are higher than those estimated by [16], which could be attributed to both different organs and different methods used. This discrepancy could be clarified by further research on cervical epithelia using the methods described in Section 2. In addition, the anisotropy factors of precancerous regions are statically higher than normal epithelia in the current study. A similar trend that the anisotropy factors of prostate tumors are greater than those of normal tissue has been reported in a previous study [10].

Knowing approximately the difference in scattering coefficients between normal and precancerous epithelia is very helpful in developing non-invasive diagnostic tools focused on quantifying the scattering coefficients of the epithelium *in vivo*. For example, for developing diffuse reflectance spectroscopy techniques, an error similar to 20% in the estimated epithelial scattering coefficient [22] would be sufficient to distinguish precancerous tissue from normal tissue. The observed high interpatient variability suggests a strategy of quantifying the epithelial scattering coefficients of normal regions on the same patient and identifying suspect lesions based on the relative change in scattering coefficients rather than using a fixed cut-off scattering coefficient for distinguishing precancerous tissue in all patients.

#245779 Received 10 Jul 2015; revised 28 Aug 2015; accepted 31 Aug 2015; published 3 Sep 2015

In summary, we estimated the scattering coefficients of fresh esophageal epithelia from quantitative phase images of thin tissue slices. The effects of fixation and paraffin embedding on tissue volume and RI were compensated for. The results show that precancerous epithelia have 37.8% higher average scattering coefficients than normal epithelia in the same patient. The increased scattering coefficient is highly correlated with increased cell density and N/C which are commonly used indicators in histopathology for diagnosing precancerous lesions. Therefore, the scattering coefficient could be a biomarker for precancerous lesions and has the potential to be quantified *in vivo*. The study provides useful guidelines for the development of *in vivo* diagnostic optical techniques using the scattering coefficient as a biomarker.

Acknowledgments

The authors thank the National Health Research Institutes (Grant No. NHRI-EX102-10020EC) and Ministry of Science and Technology (Grant No. 102-2221- E-002-032-MY3 and 102-2628-B-002 –033 -MY3) in Taiwan for financial support.

#245779 Received 10 Jul 2015; revised 28 Aug 2015; accepted 31 Aug 2015; published 3 Sep 2015